Small-strain stiffness of liquefiable sands: a comparison between bender elements and resonant-column tests

Fausto Molina-Gómez[1#], *António* Viana da Fonseca[1], *Cristiana* Ferreira[1] and *Javier* Camacho-Tauta[2]

[1]*CONSTRUCT-GEO, Universidade do Porto (FEUP), Rua Dr. Roberto Frias s/n, Porto, Portugal*
[2]*Universidad Militar Nueva Granada, Faculty of Engineering, Cra. 11 101-80, Bogotá, Colombia*
[#]*Corresponding author: fausto@fe.up.pt*

ABSTRACT

Soil stiffness can be estimated by geophysical and dynamic testing methods. In the laboratory, the most common methods to measure the small-strain stiffness are the bender elements (BE) and resonant-column (RC) tests. This paper focuses on the comparison between the results of the small-strain stiffness of sands by BE and RC tests. For this purpose, an experimental program involving three liquefiable sandy soils (i.e., NB, TP-Lisbon and Toyoura sands) was carried out. Such program covered the measurement of the small-strain stiffness of these soils by BE in triaxial and RC apparatuses for different mean effective stress conditions. All tests were carried out on saturated soil specimens, which were remoulded using the air pluviation method for various relative densities. The experimental results were interpreted in terms of shear-wave velocity (Vs) and maximum shear modulus (G_{max}) to derive the stress-dependency laws of these parameters. The experimental results revealed differences between Vs obtained from BE and RC tests, evidencing a clear effect of relative density on the shear-wave propagation. However, such a variation may be significantly reduced when a normalisation of G_{max} in terms of a void ratio function $F(e)$ is applied. As a result, this study demonstrated and validated the importance of accounting for the soil state conditions, for adequate compatibility of BE and RC tests in the estimate of the small-strain stiffness of liquefiable sands.

Keywords: Soil stiffness; Shear wave velocity; Shear modulus; Laboratory tests.

1. Introduction

The evaluation of soil stiffness is one of the major issues in geotechnical earthquake engineering. Bender elements (BE) and resonant-column (RC) tests are the most common non-destructive techniques to assess the stiffness of soils. The BE test uses a pair of piezoelectric ceramic transducers to transmit or receive a mechanical disturbance, from which the measurement of the shear-wave velocity (Vs) can be made. Such disturbance is generated by a voltage signal in the BE transmitter and detected by the BE receiver that converts it into another voltage signal. The piezoelectric transducers for BE testing can be incorporated into numerous testing devices, such as triaxial cells, simple shear devices and oedometers. The RC is recognised worldwide as the reference laboratory testing method to assess the small-strain behaviour of soils (see the standard ASTM D4015).

BE testing typically induces shear strains (γ) in the soil in the very small-strain range, below 10^{-6} (Rio, 2006), reporting values of maximum shear modulus (G_{max}) more reliably than RC testing. Nevertheless, in numerous tests, the elastic range of soils can be observed in the shear strain range between 10^{-6} and 10^{-5} (Vucetic, 1994), which corresponds to the minimum strain induced by numerous RC devices. More recently, RC devices have been equipped with BE allowing for properly and complementarily characterising the soil stiffness (Ferreira et al. 2007; Camacho-Tauta et al. 2015). Such a characterisation can be attributed to the strain level that BE and RC applied during testing. However, the devices that combine BE and RC testing (RC+BE) are unusual in geotechnical laboratory facilities. Notwithstanding, this a practice that have been common to obtain a complete characterisation of the dynamic behaviour of soils (Dyvik and Madshus, 1985). For these reasons, it is common in numerous experimental programmes to complement RC results using BE tests conducted using devices with separate configurations, e.g. triaxial cells (Viggiani and Atkinson 1995; Viana da Fonseca et al. 2009; Valle-Molina and Stokoe 2012; Astuto et al. 2022), oedometers (Lee and Santamarina 2005; Zhao et al. 2019), centrifuge apparatuses (Suits et al., 2010) or shaking table devices (Eseller-Bayat et al., 2013).

This paper focuses on comparing small-strain stiffness results using BE and RC tests on three liquefiable sands. All soil specimens were consolidated under different mean effective stresses to estimate the laws that describe the evolution of the small-strain stiffness of liquefiable sands. These tests were conducted in a collaborative program involving different testing equipment in three laboratories. The results are validated using data obtained in a RC device equipped with BE (RC+BE) in a reference sand, that is, Toyoura sand. The analysis of the results indicated a good correspondence between BE and RC tests, but only after normalising G_{max} in terms of soil state by a void ratio function. The comparison between BE and RC results demonstrated that both testing methods allow for a reliable characterisation of small-strain stiffness in liquefiable sands.

2. Materials and methods

2.1. Tested soils

The soils examined in this study cover three liquefiable sands, namely NB sand, TP-Lisbon sand and a reference sand, namely Toyoura sand. NB sand is an alluvial soil collected in the North of the Benavente municipality, located in the Lower Tagus Valley region at the south of Portugal (Ramos et al., 2019). This region has been recurrently affected by soil liquefaction phenomena, namely after the 1909 earthquake (Azevedo et al., 2010; Ferreira et al., 2020; Lai et al., 2020). TP-Lisbon sand corresponds to the liquefiable soil layer below the 'Terreiro do Paço' zone —courtyard palace, in English—located in the historical centre of Lisbon next to the Tagus River (Molina-Gómez and Viana da Fonseca, 2021). This soil experienced earthquake-induced liquefaction after the historical 1755 Lisbon earthquake, occurred on the 1st of November (All Saints day) of 1755, with a magnitude of 8.5 (Oliveira 2008; Viana da Fonseca et al. 2022). Toyoura sand is a well-known and well-characterised Japanese soil used worldwide for numerous studies about the behaviour of granular materials (e.g. Verdugo and Ishihara 1996; Liu and Yang 2018), serving as a reference material for this study.

Figure 2 shows the particle size distribution (PSD) of the liquefiable sands used in this study. The PSD were estimated by applying the ASTM procedure D6913. From Figure 2, it can be observed that the three sands have fines content (FC) below 5%. All sands were classified as sand poorly graded (SP). This classification was obtained by estimating the values of coefficient of curvature (*Cc*) and coefficient of uniformity (*Cu*). Table 1 shows the physical properties of the three examined sands. The properties in this table include the specific gravity of solid particles, *Gs*, (ASTM procedure D854); the maximum void ratio, e_{max}, (Method A of ASTM procedure D4254); the minimum void ratio (e_{min}), which was estimated using an electromagnetic vibrating table and following Method 1A of the standard ASTM procedure D4253. Furthermore, Table 1 presents the *Cc* and *Cu* values of all sands.

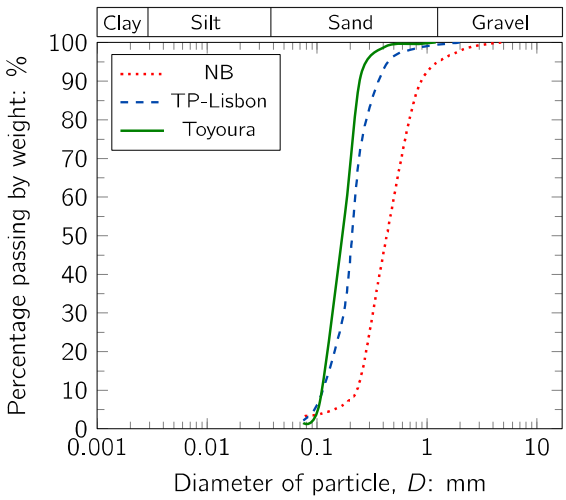

Figure 1. Particle size distribution of examined sands

Table 1. Physical properties of examined sands

Parameter	NB	TP	Toyoura
Specific gravity, *Gs*	2.64	2.66	2.64
Maximum void ratio, e_{max}	0.84	1.01	0.97
Minimum void ratio, e_{min}	0.54	0.64	0.62
Fines content, FC (%)	2.86	2.21	0.03
Mean diameter, D_{50} (mm)	0.43	0.21	0.16
Coefficient of curvature, *Cc*	0.90	1.13	0.98
Coefficient of uniformity, *Cu*	2.16	1.69	1.46

2.2. Testing devices

In this study, bender element (BE) and resonant-column (RC) tests were conducted to estimate the dynamic properties of liquefiable sands. The testing apparatuses belong to three different laboratories, that is, Geotechnical Laboratory of the Faculty of Engineering of the University of Porto (Porto, Portugal), the Center for Studies in Road Infrastructure and Geotechnics of the Nueva Granada Military University (Bogota, Colombia) and the Laboratory of Geotechnics of the University of Lisbon (Lisbon, Portugal).

The BE tests were carried out in the Geotechnical Laboratory of the University of Porto (labGEO) using a conventional triaxial cell equipped with a pair of identical piezoceramic transducers, which were installed in the base and top caps of such cell. The tests set-up consists of a GDS pressure/volume control panel, a function generator (TTi TG1010), an output amplifier (designed at the University of Western Australia), an oscilloscope (Tektronix TDS 220) and a computer with WaveStar software to acquire the wave signals. The RC tests were carried out in the Center for Studies in Road Infrastructure and Geotechnics of the Universidad Militar Nueva Granada. This RC apparatus is of bottom-fixed and top-free configuration or Stokoe-type manufactured by Wykeham Farrance. This apparatus has an internal function generator with a digital interface, controlled through the apparatus software, which can generate different types of voltage signals to the coils attached to the cell body. The pressure during testing was applied by a pneumatic, which was controlled automatically by the apparatus software. The instrumentation of this device included an axial Linear Variable Displacement Transducer (LVDT), three pressure transducers, a volume change gauge, and two MEMS accelerometer.

On the other hand, an RC apparatus equipped with BE elements (RC+BE) was also used. The tests with this configuration were carried out in the Laboratory of Geotechnics of the University of Lisbon. The RC apparatus of this laboratory covers a Drnevich-type configuration manufactured by Seiken Inc., which incorporates three subsystems: pneumatic, electro-mechanic and electronic. The pneumatic subsystem allowed for controlling cell pressure, backpressure and axial force; the electro-mechanical subsystem applied the torsional vibration; and the electronic subsystem provided the input signal and measured the system response. The BE of this system comprised a pair of piezoceramic transducers installed in the base and top platens of the RC apparatus. The setup of the BE included

a switching box (manufactured by UWA) to select/change the sensor used in the test and an electronic filter/amplifier (Krohn-Hite, model 3384) to obtain a stronger output signal. Both BE and RC signals were generated and acquired using LabVIEW software tools specifically adapted for this equipment (Camacho-Tauta, 2011). Figure 2 shows the three apparatuses used in this study.

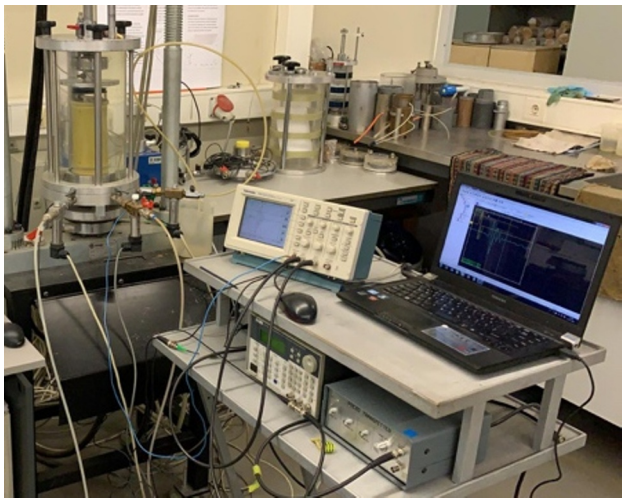

a)

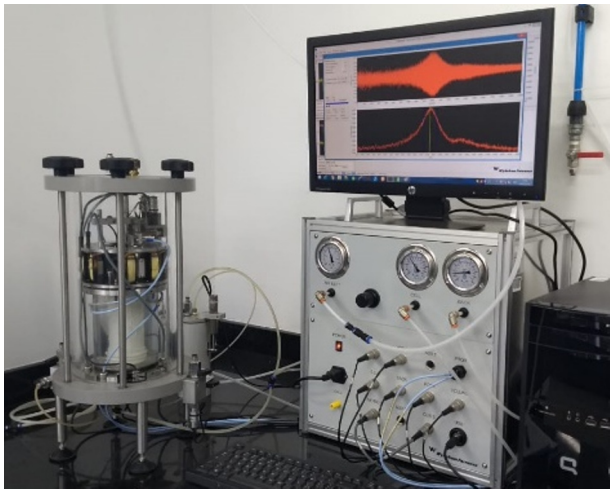

b)

c)

Figure 2. Different geotechnical apparatuses used in this study: a) BE setup at labGEO; b) RC at the Nueva Granada Militar University; c) RC equipped with BE at the University of Lisbon

2.3. Experimental procedures

Soil specimens of NB, TP-Lisbon and Toyoura sands were remoulded for different values of relative density (*Dr*). The *Dr* values for NB sand and TP-Lisbon sand were selected to match the natural in-situ conditions, using the correlation of the CPT tests proposed by Robertson (2009), as indicated in Molina-Gómez et al. (2020). The soil remoulding was performed by applying the air pluviation method (Ishihara, 1996). All soil specimens were saturated using the procedures recommended by Viana da Fonseca et al. (2021). The soil specimens were only considered completely saturated if Skempton's *B*-value was higher than 0.97. After validating the full saturation condition, the soil specimens were isotropically consolidated under mean effective stress (p') between 20 kPa and 500 kPa to define the stress-dependency law of these liquefiable sands using the different apparatuses. At the end of the test, the samples were carefully removed, avoiding any loss of soil or water (Viana da Fonseca et al. 2021). The end-of-test void ratio (e_f) was estimated by computing:

$$e_f = \frac{Gs \cdot \omega_f}{Sr} \quad (1)$$

where ω_f is the final water content, and the degree of saturation (*Sr*) was considered 100% since *B*-values greater than 0.97 were reported in all tests. The relative density during testing was computed based on the e_f, e_{max} and e_{min} values.

For the BE tests, sinusoidal pulses at different frequencies were used as input signals to excite the BE transmitter. The wave propagation travel time (t_t) was obtained using the first arrival method (Lee and Santamarina, 2005). To minimise the uncertainty and subjectivity associated with the interpretation of BE test results, associated with cross-talk or near-field effect, four input signals with frequencies between 1-8 kHz were applied (Viana da Fonseca et al. 2009). Figure 3 shows the typical results of BE tests for different input frequencies and interpreted using the first arrival time method.

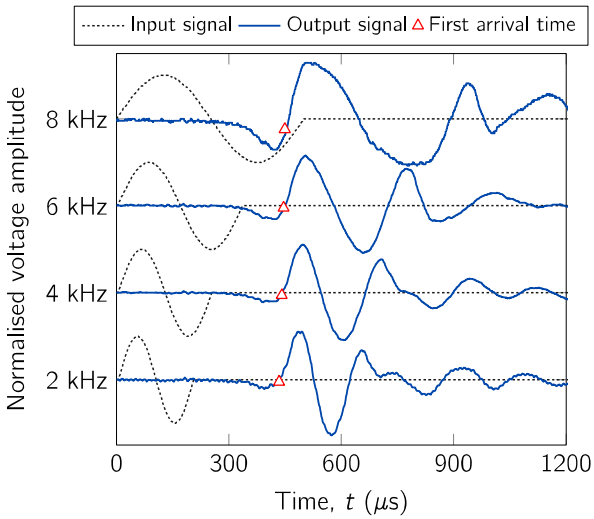

Figure 3. Typical signals reported during BE testing –results on TP-Lisbon sand under p' = 500 kPa

For the RC tests, in the apparatuses at the Nueva Granada Militar University and the University of Lisbon, a sine-sweep signal, with frequencies between 60 Hz to 120 Hz and an amplitude of 1 mV or 2mV, was applied to identify the resonant frequency of the system. The measurements were conducted eleven times to clean by averaging the output response contaminated by electrical noise. During these tests, the low-amplitude excitation signals generated strain (γ) values in the range of 10^{-5}. The signals were interpreted using the transfer function (H) described as follows (Santos, 1999):

$$H = \frac{\theta_0}{T_0} e^{-i\phi} = \frac{J\omega^2}{\left(\frac{\omega h}{V_S^*}\right) tan\left(\frac{\omega h}{V_S^*}\right)} - J_A\omega^2 + J_A{\omega_A}^2(1 + i2\xi_A) \quad (2)$$

where θ_0 and T_0 are rotation and torque amplitudes for different angular frequencies ω, ϕ is phase angle between them; h and J are the length and rotation mass inertia of the specimen, respectively. J_A, ξ_A and ω_A are the calibration factors of the active end, that is, rotational mass inertia, damping ratio and angular resonant frequency, respectively. Besides, $V_S^* = V_S\sqrt{1 + i2\xi}$ is the complex shear-wave velocity where ξ is the damping ratio of the soil and $i = \sqrt{-1}$. The transfer function data can be obtained through experimental modal analysis techniques (Khan et al. 2011) from several time series. Vibration data of torque (T) and rotation (θ) along time (t) from sine sweep tests is recorded and the transfer function is computed by:

$$H(\omega) = \frac{\mathcal{F}\{\theta(t)\} \cdot \overline{\mathcal{F}\{T(t)\}}}{\mathcal{F}\{T(t)\} \cdot \overline{\mathcal{F}\{T(t)\}}} \quad (3)$$

where $\mathcal{F}\{\ \}$ is the Fourier transform operator and bar over function means the complex conjugate function. The transfer function is an average of eleven measurements to cancel the external noise. A curve fitting of the complex data obtained from experiments using Eq. 3 provides the unknown soil parameters of the right side of Eq. 2, namely the shear-wave velocity *Vs* and the damping ratio ξ. Due to the complex components, solving for V_S^* requires an iterative procedure in complex variables which needs initial estimated values of the soil properties, i.e. *Vs* and ξ. This method is suitable for characterising small-strain stiffness, in which the soil behaves linearly.

Figure 4 shows the typical experimental results and a comparison against the theoretical response obtained by the computation of the transfer function (see Eq. 2). This figure presents the system response variation as a function of the different frequencies of the sine-sweep signal during RC testing. In all RC tests, the resonant frequency (ω_R) was defined as the frequency for the maximum absolute value of transfer function ($|H|$). At this point, the transfer function exhibited a sharp peak, which allowed defining the resonant point (92 Hz in Figure 4). The resonant point was confirmed by the phase angle (ϕ), which must be equal to -π/2 rad at ω_R (Khan et al. 2011). Moreover, in Figure 4, it can be observed a good agreement between device measurements and the theoretical solution. However, in the low and high frequencies of the sine-sweep signal, the phase showed some scatter in Figure 4.b, which did not influence the identification of ω_R.

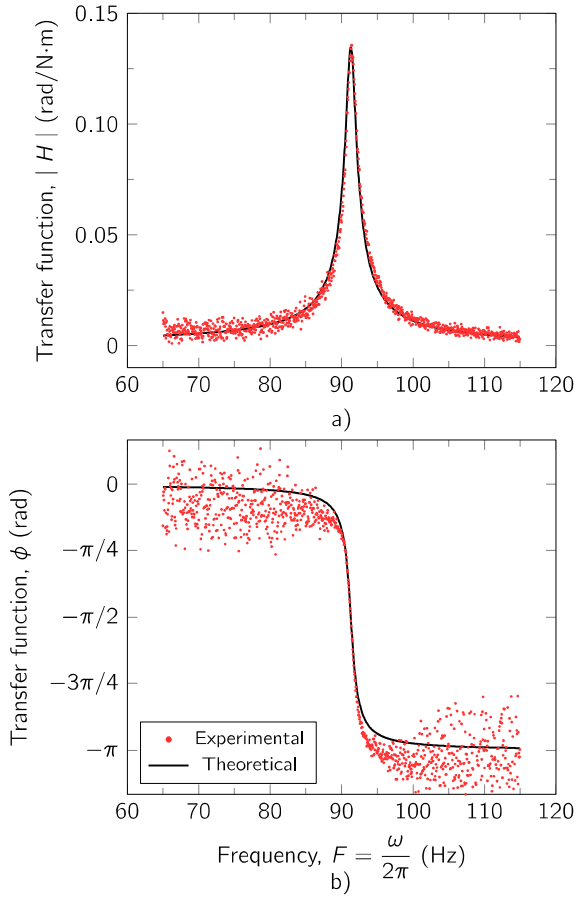

Figure 4. Typical experimental results compared against the transfer function computation –test in NB sand at p'=100 kPa and $\gamma = 7.11\times10^{-6}$: a) magnitude; b) phase

3. Analysis of results and discussion

This section presents the results and analysis of the BE, RC and RC+BE tests. Table 2 indicates the test conditions of this study. From Table 2, it can be observed that all the tests were carried out under different mean effective stresses (p') and various relative densities (Dr), except one soil specimen of Toyoura sand, which was tested in the improved RC+BE apparatus at the University of Lisbon.

Table 2. Test conditions of soil specimens

Sand	Test-type	*e* (-)	*Dr* (%)	*p'* (kPa)
NB	BE	0.73	38	20; 50; 150; 300; 500
NB	BE	0.77	23	30; 50; 100; 150; 200
NB	RC	0.71	42	30; 50; 100; 150; 200
TP	BE	0.91	28	20; 50; 150; 300; 500
TP	BE	0.72	77	20; 50; 100; 200; 400
TP	RC	0.88	33	30; 50; 100; 150; 200
Toyoura	BE	0.75	61	20; 50; 100; 200; 400
Toyoura	RC+BE	0.69	81	100; 200; 400

Experimental results showed that the mean effective stress (p') affected the shear-wave propagation in

liquefiable sands, inducing a faster wave propagation at higher p' values. Figure 5 presents the typical results of shear-wave propagation measured by BE testing. From Figure 5, a reduction of the shear-wave travel time as p' increases can be confirmed.

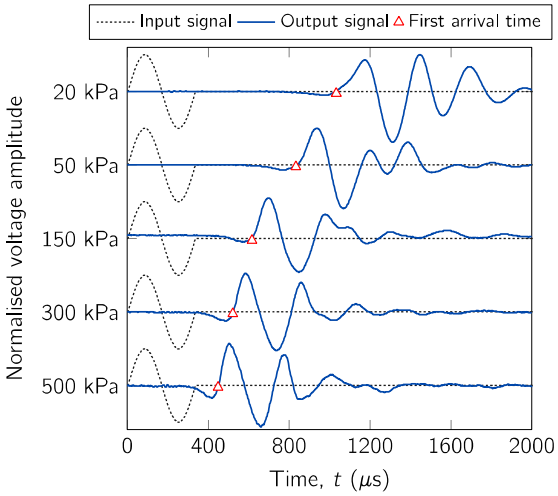

Figure 5. Typical BE results for different p' values –tests in TP-Lisbon sand using 4 kHz input signal frequency

The variation of the shear-wave arrival time for different p' values revealed a clear effect or stress-dependency on S-wave propagation. These effects were analysed by estimating the variation of the shear-wave velocity (Vs) as a function of p'. Vs was computed by the ratio between the tip-to-tip distance of BE (L_{tt}) and the wave propagation time (t_t), as suggested by diverse authors (e.g. Viana da Fonseca et al. 2009; Camacho-Tauta et al. 2015; Yamashita et al. 2009; Viggiani and Atkinson 1995).

Figure 6 presents the results of the stress-dependency of Vs in all examined sands. BE tests have been analysed to derive the best fit of the stress dependency law using the general form:

$$Vs = \alpha\,(p')^{\beta} \tag{3}$$

where α corresponds to the Vs value at 1 kPa, and β is the exponent of the stress-state dependency law that describes the evolution of Vs. The Vs results obtained from BE tests were compared against Vs values obtained from RC tests for all liquefiable sands. All stress-dependency laws reported in Figure 6 were derived under a coefficient of determination $R^2 > 0.96$. Table 3 summarises the parameters that describe the stress-dependency laws of all sands.

Table 3. Parameters of stress-dependency laws of Vs

Sand	Test-type	α	β	R^2
NB	BE	61.93	0.26	0.98
NB	RC	71.25	0.23	0.97
NB	RC	81.15	0.24	0.97
TP	BE	65.68	0.25	0.99
TP	BE	98.43	0.24	0.98
TP	RC	81.39	0.25	0.98
Toyoura	BE	72.61	0.22	0.98
Toyoura	BE*	106.16	0.17	0.96
Toyoura	RC*	106.67	0.18	0.97

* Tests conducted in the RC+BE equipment

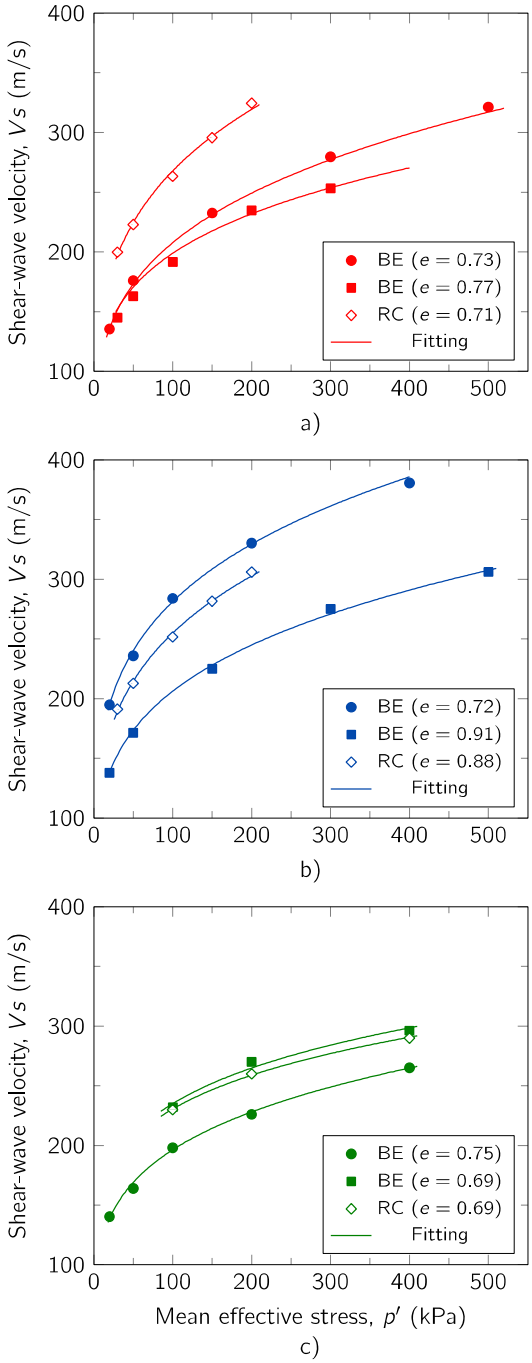

Figure 6. Stress-dependency of Shear-wave velocity: a) NB sand; b) TP-Lisbon sand; c) Toyoura sand

From Figure 6, it can be observed that the stress-dependency laws derived from both testing procedures are parallel. Besides, Figure 6 indicates differences between BE and RC results, exhibiting higher Vs values in RC tests for NB sand. For the case of TP-Lisbon sand, RC is between the two BE results at higher and lower e. These differences can be attributed to variations in the relative density of the soil specimens, which were different for these tests. Figure 6c shows differences between BE and BE results in Toyoura sand using the RC+BE apparatus, indicating that the BE results are slightly higher than RC results. The divergence between the Vs results on Toyoura sand carried out in the RC+BE were because of the strain level induced by BE ($\gamma<10^{-6}$), which is lower than the strains induced during RC testing, as demonstrated experimentally by laser and

accelerometer measurements (Camacho-Tauta et al., 2015; Irfan et al., 2020). Besides, the slightly higher *Vs* values of BE results in the BE+RC apparatus could be attributed to the frequency effects on wave propagation, as validated theoretically by Biot (1956), which tends to increase when apply higher frequencies.

Although the *Vs* allows for characterising the small-strain stiffness of granular materials due to the direct estimation by several in situ and laboratory testing, this parameter is not used as an input parameter in numerical analyses. Therefore, the maximum shear modulus (G_{max}) derived from equation 4 was also used herein to describe the small-strain stiffness of the liquefiable sands. Equation 4 relates the mass density (ρ) with the shear-wave velocity (*Vs*).

$$G_{max} = \rho\, Vs^2 \tag{4}$$

However, the small-strain stiffness is strongly dependent on the void ratio (e), as demonstrated in Figure 6. Hence, G_{max} is higher for dense sands, i.e. lower e values. The void ratio functions, $F(e)$, allow eliminating the effect of soil state on G_{max}. Lo Presti et al. (1997) proposed an exponential $F(e) = e^{-1.29}$ based on Hertz's theory, which relates the arrangement of particles to the G_{max} changes. This model was applied to normalise the BE and RC results reported in Figure 6 in terms of the void ratio referred in Table 2. Figure 7 compares the stress-dependency of the maximum shear modulus (G_{max}) and normalised shear modulus ($G_{max}/F(e)$).

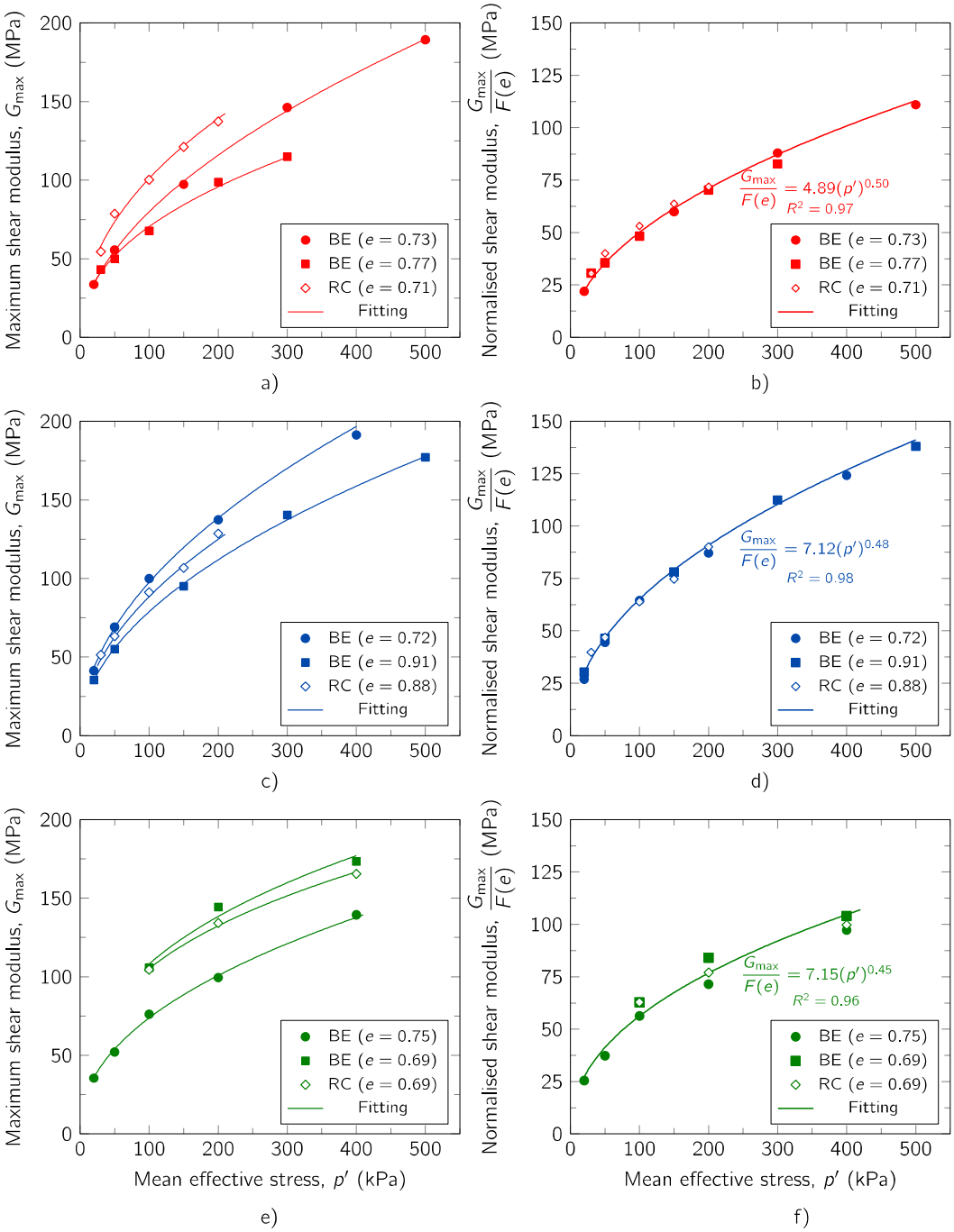

Figure 7. Stress-dependency of maximum shear modulus and normalised shear modulus: a) and b) NB sand; c) and d) TP-Lisbon sand; e) and f) Toyoura sand

Figure 7 reveals a good agreement between the $G_{max}/F(e)$ results obtained from both BE and RC tests. From Figure 7, it can be observed that a single law describes well the stress-dependency of normalised shear modulus results for each sand. These results confirmed that the differences between the stress-dependency laws of *Vs* were effectively due to differences in relative density, which affects the small-strain stiffness of liquefiable sands. Moreover, small differences between the BE and RC results were detected for tests conducted under the same p'. The differences between the experimental results and curve fitting of $G_{max}/F(e)$ ranged from 1% to 9%. Such findings can be validated by the results reported in Figures 7b, 7d and 7f, which indicated similar $G_{max}/F(e)$ results for both BE and RC tests. Therefore, it can be concluded that the void ratio normalisation allows for characterising well the small-strain stiffness of a specific soil at different densities conditions using both testing procedures.

4. Conclusion

This paper has compared a series of small-strain stiffness results of three liquefiable sands (NB sand, TP-Lisbon sand and Toyoura sand) using bender elements and resonant-column tests. The experimental program included measurements of shear-wave velocity, from which normalised maximum shear modulus under different effective confining stresses were determined. Stress-dependency laws of shear-wave velocity were derived from bender elements and resonant-column testing. Results indicated that the laws obtained from resonant-column tests were higher than the laws obtained from Bender Element tests. These differences were attributed to the effects of relative density of soil specimens. In this sense, a normalisation of shear modulus using a void ratio function can be used to converge the results obtained from both testing procedures. This normalisation provided a reliable comparison, which demonstrated a good agreement between all results. The comparison revealed an error lower than 10%. The findings of this approach were validated by tests in a reference soil, namely Toyoura sand, conducted in a resonant-column apparatus improved with bender elements. Slightly differences were observed between resonant-column and bender element tests. These differences were attributed to the strain level induced in each testing procedure, which is lower in the bender element tests. Therefore, by following accurate testing procedures and by measuring properly the soil state (i.e. the void ratio), it is possible to obtain a characterisation of the small-strain stiffness of liquefiable sands by using different apparatuses in different laboratories.

Acknowledgements

This work was financially supported by UIDB/04708/2020 and UIDP/04708/2020 of CONSTRUCT – Institute of R&D in Structures and Construction, Portugal funded by the national funds through the FCT/MCTES (PIDDAC). The Vice President Office for Research of the Universidad Militar Nueva Granada funded the project under grant number IMP-ING-2932. The first author acknowledges the support of FCT through the grant SFRH/BD/146265/2019. The authors also acknowledge the technical support given by Eng Daniela Coelho and Mr. Armando Pinto of LabGEO, and Eng Sebastián Roldán of UMNG during the development of the experimental program presented herein.

References

ASTM International, 2017. ASTM D6913/D6913M - 17 Standard Test Methods for Particle-Size Distribution (Gradation) of Soils Using Sieve Analysis.

ASTM International, 2016a. D4254 - Standard Test Methods for Minimum Index Density and Unit Weight of Soils and Calculation of Relative Density.

ASTM International, 2016b. D4253 - Test Methods for Maximum Index Density and Unit Weight of Soils Using a Vibratory Table.

ASTM International, 2014a. D4015 - Standard Test Methods for Modulus and Damping of Soils by Resonant-Column.

ASTM International, 2014b. D854 - Standard Test Methods for Specific Gravity of Soil Solids by Water Pycnometer.

Astuto, G., Molina-Gómez, F., Bilotta, E., Viana da Fonseca, A., Flora, A., 2023. Some remarks on the assessment of P-wave velocity in laboratory tests for evaluating the degree of saturation. Acta Geotech. 18, 777–790. https://doi.org/10.1007/s11440-022-01610-9

Azevedo, J., Guerreiro, L., Bento, R., Lopes, M., Proença, J., 2010. Seismic vulnerability of lifelines in the greater Lisbon area. Bull. Earthq. Eng. 8, 157–180. https://doi.org/10.1007/s10518-009-9124-7

Biot, M.A., 1956. Theory of Propagation of Elastic Waves in a Fluid-Saturated Porous Solid II. Higher Frequency Range. J. Acoust. Soc. Am. 28, 179–191. https://doi.org/10.1121/1.1908241

Camacho-Tauta, J., 2011. Evaluation of the small-strain stiffness of soil by non-conventional dynamic testing methods. Universidade de Lisboa.

Camacho-Tauta, J., Cascante, G., Viana da Fonseca, A., Santos, J.A., 2015. Time and frequency domain evaluation of bender element systems. Géotechnique 65, 548–562. https://doi.org/10.1680/geot.13.P.206

Dyvik, R., Madshus, C., 1985. Lab Measurements of Gmax Using Bender Elements, in: Advances in the Art of Testing Soils Under Cyclic Conditions. ASCE.

Eseller-Bayat, E., Gokyer, S., Yegian, M.K., Deniz, R.O., Alshawabkeh, A., 2013. Bender Elements and Bending Disks for Measurement of Shear and Compression Wave Velocities in Large Fully and Partially Saturated Sand Specimens. Geotech. Test. J. 36, 20120024. https://doi.org/10.1520/GTJ20120024

Ferreira, C., Viana da Fonseca, A., Ramos, C., Saldanha, A.S., Amoroso, S., Rodrigues, C., 2020. Comparative analysis of liquefaction susceptibility assessment methods based on the investigation on a pilot site in the greater Lisbon area. Bull. Earthq. Eng. 18, 109–138. https://doi.org/10.1007/s10518-019-00721-1

Ferreira, C., Viana da Fonseca, A., Santos, J.A., 2007. Comparison of Simultaneous Bender Elements and Resonant Column Tests on Porto Residual Soil. pp. 523–535. https://doi.org/10.1007/978-1-4020-6146-2_34

Irfan, M., Cascante, G., Basu, D., Khan, Z., 2020. Novel evaluation of bender element transmitter response in transparent soil. Geotechnique 70, 187–198. https://doi.org/10.1680/jgeot.17.P.256

Ishihara, K., 1996. Soil Behaviour in Earthquake Geotechnics, 1st ed. Clarendon Press, Oxford.

Khan, Z., El Naggar, M.H., Cascante, G., 2011. Frequency

dependent dynamic properties from resonant column and cyclic triaxial tests. J. Franklin Inst. 348, 1363–1376. https://doi.org/10.1016/J.JFRANKLIN.2010.04.003

Lai, C.G., Bozzoni, F., Conca, D., Famà, A., Özcebe, A.G., Zuccolo, E., Meisina, C., Bonì, R., Bordoni, M., Cosentini, R.M., Martelli, L., Poggi, V., Viana da Fonseca, A., Ferreira, C., Rios, S., Cordeiro, D., Ramos, C., Molina-Gómez, F., Coelho, C., Logar, J., Maček, M., Oblak, A., Ozcep, F., Bozbey, I., Oztoprak, S., Sargin, S., Aysal, N., Oser, C., Kelesoglu, M.K., 2020. Technical guidelines for the assessment of earthquake induced liquefaction hazard at urban scale. Bull. Earthq. Eng. 1–45. https://doi.org/10.1007/s10518-020-00951-8

Lee, J.-S., Santamarina, J.C., 2005. Bender Elements: Performance and Signal Interpretation. J. Geotech. Geoenvironmental Eng. 131, 1063–1070. https://doi.org/10.1061/(ASCE)1090-0241(2005)131:9(1063)

Liu, X., Yang, J., 2018. Shear wave velocity in sand: effect of grain shape. Géotechnique 68, 742–748. https://doi.org/10.1680/jgeot.17.T.011

Lo Presti, D.C.F., Jamiolkowski, M., Pallara, O., Cavallaro, A., Pedroni, S., 1997. Shear modulus and damping of soils. Géotechnique 47, 603–617. https://doi.org/10.1680/geot.1997.47.3.603

Molina-Gómez, F., Viana da Fonseca, A., 2021. Key geomechanical properties of the historically liquefiable TP-Lisbon sand. Soils Found. 61, 836–856. https://doi.org/10.1016/j.sandf.2021.03.004

Molina-Gómez, F., Viana da Fonseca, A., Ferreira, C., Camacho-Tauta, J., 2020. Dynamic properties of two historically liquefiable sands in the Lisbon area. Soil Dyn. Earthq. Eng. 132, 106101. https://doi.org/10.1016/j.soildyn.2020.106101

Oliveira, C.S., 2008. Review of the 1755 Lisbon Earthquake Based on Recent Analyses of Historical Observations, in: Fréchet, J., Meghraoui, M., Stucchi, M. (Eds.), Historical Seismology: Interdisciplinary Studies of Past and Recent Earthquakes. Springer, pp. 261–300. https://doi.org/10.1007/978-1-4020-8222-1_13

Ramos, C., Ferreira, C., Molina-Gómez, F., Viana da Fonseca, A., 2019. Critical State Lines of Portuguese liquefiable sands. E3S Web Conf. 92, 06003. https://doi.org/10.1051/e3sconf/20199206003

Rio, J.F., 2006. Advances in laboratory geophysics using bender elements. University College of London.

Robertson, P.K., 2009. Interpretation of cone penetration tests - a unified approach. Can. Geotech. J. 46, 1337–1355. https://doi.org/10.1139/T09-065

Santos, J.A., 1999. Soil characterization by dynamic and cyclic torsional shear test. Application to study of piles under static and dynamic horizontal loading (in portuguese). Universidade de Lisboa.

Suits, L.D., Sheahan, T.C., Kim, N.-R., Kim, D.-S., 2010. A Shear Wave Velocity Tomography System for Geotechnical Centrifuge Testing. Geotech. Test. J. 33, 102894. https://doi.org/10.1520/GTJ102894

Valle-Molina, C., Stokoe, K.H., 2012. Seismic measurements in sand specimens with varying degrees of saturation using piezoelectric transducers. Can. Geotech. J. 49, 671–685. https://doi.org/10.1139/t2012-033

Verdugo, R., Ishihara, K., 1996. The Steady State of Sandy Soils. Soils Found. 36, 81–91. https://doi.org/10.3208/sandf.36.2_81

Viana da Fonseca, A., Cordeiro, D., Molina-Gómez, F., 2021. Recommended Procedures to Assess Critical State Locus from Triaxial Tests in Cohesionless Remoulded Samples. Geotechnics 1, 95–127. https://doi.org/10.3390/GEOTECHNICS1010006

Viana da Fonseca, A., Ferreira, C., Fahey, M., 2009. A Framework Interpreting Bender Element Tests, Combining Time-Domain and Frequency-Domain Methods. Geotech. Test. J. 32, 100974. https://doi.org/10.1520/GTJ100974

Viana da Fonseca, A., Molina-Gómez, F., Ferreira, C., 2023. Liquefaction resistance of TP-Lisbon sand: a critical state interpretation using in situ and laboratory testing. Bull. Earthq. Eng. 21, 767–790. https://doi.org/10.1007/s10518-022-01577-8

Viggiani, G., Atkinson, J.H., 1995. Interpretation of bender element tests. Geotechnique 45, 149–154. https://doi.org/10.1680/geot.1997.47.4.873

Vucetic, M., 1994. Cyclic Threshold Shear Strains in Soils. J. Geotech. Eng. 120, 2208–2228. https://doi.org/10.1061/(ASCE)0733-9410(1994)120:12(2208)

Yamashita, S., Kawaguchi, T., Nakata, Y., Mikamt, T., Fujiwara, T., Shibuya, S., 2009. Interpretation of international parallel test on the measurement of G max using bender elements. Soils Found. 49, 631–650. https://doi.org/10.3208/sandf.49.631

Zhao, Y., Mahmood, N.S., Coffman, R.A., 2019. Small-Strain and Large-Strain Modulus Measurements with a Consolidation Device. J. Test. Eval. 47, 20160331. https://doi.org/10.1520/JTE20160331